Pramāṇa – J. Phys., Vol. 28, No. 2, February 1987, pp. 117–130. © Printed in India.

Analytic representation for ^{3}He form factors

K N AGRAWALLA and M K PARIDA*

Kendrapara College, Kendrapara, Cuttack 754 211, India
*Physics Department, North Eastern Hill University, Shillong 793 003, India

MS received 14 March 1986; revised 5 November 1986

Abstract. A modified N/D method is applied for the cases of ^{3}He charge and magnetic form factors. Anomalous cut positions are computed using possible exchanges at the photon-^{3}He electromagnetic vertex, and one of them is found at $t_a = 0{\cdot}0618$ GeV^2. The D-function is used to parametrize the two-pion cut while the N-function is taken to represent the effect of an anomalous or the three-pion cut. Excellent fits to the available experimental data on charge and magnetic form factors are obtained and several useful information on the form factors computed.

Keywords. Analytic representation; modified N/D method; ^{3}He form factors.

PACS Nos 13·40; 11·50; 25·30

1. Introduction

A modified N/D method of analytic representation of electromagnetic form factors was found to be very successful in parametrizing the experimental data on pion and nucleon form factors and obtaining useful information about them (Deo and Parida 1973, 1974; Deo 1974). In this method, the nearest normal cut contribution in the t-plane was represented by the D function and an effective range type of formula, obtainable from dispersion relation, but the next nearest normal-cut contribution was assumed to be represented by the N-function approximated by optimized polynomial expansion in a suitably chosen conformally mapped variable, Z, which maps the cut in the t plane onto the boundary of a parabola in the Z plane (Cutkosky and Deo 1968; Ciulli 1969; Deo and Parida 1971). Further modifications have been suggested in order that this approach be applicable for the form factors of light nuclei (Parida 1979; Parida *et al* 1983; Agrawalla and Parida 1985). The applicability of the modified N/D method has been successfully tested for isoscalar light nuclei like deuteron and ^{4}He. In the case of the deuteron, the anomalous cut is nearer to the origin than any other cut, but computations in the case of ^{4}He revealed that all anomalous cut positions are farther away than the normal three-pion cut in t-plane (Agrawalla and Parida 1985). Parametrizing the anomalous cut contribution by the N function, and including the exponential weight function in the Laguerre polynomial expansion, have resulted in obtaining excellent fits to the data on charge and magnetic form factors of deuteron and the charge form factor of ^{4}He (Agrawalla and Parida 1985). In this paper the modified

* To whom correspondence should be addressed.

formula is applied to the cases of charge and magnetic form factors of a nonisoscalar target like ^{3}He.

In § 2 we present the working formula and compute the anomalous cut positions. In §§ 3 and 4 we present our results on the data analysis of ^{3}He magnetic and charge form factors, respectively. Our results are summarized and conclusions stated in § 5.

2. The modified N/D method and analytic structure

In this section we mention the modified N/D representation and also compute the positions of the anomalous cut using several possible exchanges at the photon-^{3}He vertex.

2.1 *The modified N/D representation*

The formula proposed for the form factor of a light nucleus is (Parida 1979; Parida *et al* 1983; Agrawalla and Parida 1985)

$$F(t) = N(t)/D(t), \tag{1}$$

where the D-function is assumed to represent the effect of the nearest normal cut, but the N-function is taken to represent the effect of an anomalous cut or the next-nearest-normal cut. The D-function is parametrized using an effective range type of formula obtainable from dispersion relation, but the N-function is approximated by optimized polynomial expansion. For ^{3}He form factors the nearest normal cut starts at $t = 4m_\pi^2$, which contributes to the D-function as (Deo and Parida 1973, 1974)

$$D(t) = \sum_n a_n t^n + h(t) + \frac{m_\pi^2}{\pi}, \tag{2}$$

where

$$h(t) = \frac{2}{\pi}\frac{k^3}{\sqrt{t}} \ln\left[\left(\frac{t}{4m_\pi^2}\right)^{1/2} + \left(\frac{t}{4m_\pi^2} - 1\right)^{1/2}\right] - i\frac{k^3}{\sqrt{t}}, \tag{3}$$

with

$$k = \left(\frac{t}{4} - m_\pi^2\right)^{1/2}. \tag{4}$$

The next nearest normal physical cut occurs at $t = 9m_\pi^2 \simeq 0{\cdot}18\ \text{GeV}^2$. This or an anomalous cut starting at $t = t_a$ can be mapped onto the boundary of a parabola in the Z plane with the physical region of the t plane being mapped onto the physical region, $0 \leqslant \text{Re}\, Z \leqslant \infty$, of Laguerre polynomial expansion whose domain of convergence is the interior of the parabola. Then (Parida 1979)

$$N(t) = \exp(-\alpha Z) \sum_l g_l L_l(2\alpha Z), \tag{5}$$

with

$$Z(t) = \left\{\ln\left[\left(\frac{-t}{t_a}\right)^{1/2} + \left(\frac{-t}{t_a} + 1\right)^{1/2}\right]\right\}^2. \tag{6}$$

Assuming that the series (5) converges sufficiently rapidly, we can rewrite the

N-function for the first M significant terms as

$$N(t) = \exp(-\alpha Z) \sum_{l=0}^{M} e_l Z^l. \tag{7}$$

Comparing (5) and (7), the relations between the unknown parameters g_l's and e_l's can be written down easily. The t dependence for the charge form factor, $F_c(t)$, or the magnetic form factor, $F_m(t)$, are given by (1)–(7) but with different sets of parameters, α, e_l, g_l, a_n and t_a for each. These sets of parameters are to be determined from data fitting to know the functions $F_c(t)$ and $F_m(t)$. Besides the N/D representation, we also use two other formulas to compute the root mean square radii

$$r_i = [6\, F_i'(0)]^{1/2}, \tag{8}$$

and the charge or magnetic moment density distribution

$$\rho_i(r) = \frac{1}{4\pi^2 r} \int_0^\infty F_i(|t|) \sin(r\sqrt{|t|})\, \mathrm{d}|t|, \tag{9}$$

where $i = c$ or m, corresponding to the charge or magnetic form factor, in (8) and (9).

2.2 *Computation of the anomalous cut positions*

We have computed the anomalous cut positions using the photon-^{3}He vertex of figure 1, where each of a, b and c stand for an exchanged particle, multiparticle, a light nucleus state like deuteron, or their combination. The most familiar exchanges correspond to these objects being deuteron, proton or neutron. The formula representing the cut position can be written as (Eden *et al* 1966; Hamilton 1968; Agrawalla and Parida 1985)

$$\begin{aligned} -t = \frac{1}{2m_c^2} [&(m_b^2 + m_c^2 - M^2)(m_c^2 + m_a^2 - M^2) \\ &\pm \{16 m_a^2 m_b^2 m_c^4 + (m_b^2 + m_c^2 - M^2)^2 (m_c^2 + m_a^2 - M^2)^2 \\ &- 4 m_b^2 m_c^2 (m_c^2 + m_a^2 - M^2)^2 - 4 m_c^2 m_a^2 (m_b^2 + m_c^2 - M^2)^2 \}^{1/2}] \\ &- (m_a^2 + m_b^2), \end{aligned} \tag{10}$$

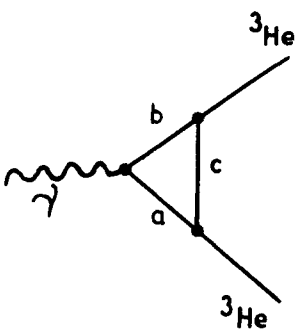

Figure 1. Vertex graph for computation of the anomalous cuts of ^{3}He form factors as described in the text.

where m_a, m_b, m_c and M represent masses of a, b, c and ^{3}He, respectively. In (10), only the plus route yields the correct anomalous-cut position as can be verified using exchanges with $a = b$. We denote the values corresponding to the plus route of (10) as t_a. In table 1 we have calculated t_a values for familiar transitions like $^3\text{He} \to p + d$, and others like $^3\text{He} \to pp + n$, $^3\text{He} \to n\pi^+ + d$, $^3\text{He} \to d + N^*$, and $^3\text{He} \to p + d\pi^0$. The nearest anomalous cut at $t_a = 0{\cdot}0618$ GeV^2 is found to occur for the simplest vertex corresponding to the transition $^3\text{He} \to p + d$ and the (a, b, c) combination (p, p, d). This cut position occurs sufficiently below the two-pion cut. The next nearest anomalous cut at $t_a = 0{\cdot}075$ GeV^2 occurs for the less familiar and plausible transition, $^3\text{He} \to pp + n$ and the (a, b, c) combination (n, n, pp) and almost coincides with the two-pion cut. A third and the next nearest anomalous cut, which exists between the three-pion and the four-pion cuts, is due to the simple (a, b, c) combination (d, d, p) and also seems plausible. Other anomalous cuts existing at more distant points in the t plane and their (a, b, c) combinations are presented in table 1. As found out by us (Agrawalla and Parida 1985) all the anomalous cuts for ^{4}He charge form factor occur above the three-pion cut, but for ^{3}He, this computation shows that there exists one anomalous cut sufficiently below the two-pion cut. Thus, whereas the nearest threshold in the t plane for ^{4}He form factor is a normal threshold, for the ^{3}He form factors it is an anomalous threshold.

3. Analysis of the magnetic form factor data and extrapolation

We have taken all the available 32 data points with their errors reported by several experimental groups (McCarthy *et al* 1977; Frosch *et al* 1967; McAllister *et al* 1956). As explained in § 2, the D-function defined through formulas (2)–(4) is used to parametrize the two-pion cut. For the sake of convenience in data fitting, the N-function is chosen in the form (7), and assumed to represent the contribution due to an anomalous cut, or a normal cut other than the two-pion cut. Setting the normalization condition on two unknown parameters as $e_0 = a_0$ and using $\alpha = 0$, which corresponds to the absence of

Table 1. Computation of anomalous-cut positions with various exchanges, a, b and c in the vertex graph of figure 1.

a	b	c	Anomalous-cut positions t_a (GeV^2)
p	p	d	0·0618
d	d	p	0·2470
n	n	pp	0·0750
pp	pp	n	0·2993
$d\pi^0$	$d\pi^0$	p	0·2573
p	p	$d\pi^0$	1·3381
$n\pi^+$	$n\pi^+$	d	1·7385
d	d	$n\pi^+$	5·2530
$p\pi^0$	$p\pi^0$	d	1·6535
d	d	$p\pi^0$	5·2015
$N^*(1470)$	$N^*(1470)$	d	3·8173
d	d	$N^*(1470)$	8·6569

the exponential weight function in the N function, yielded a very large value of total χ^2 ($\simeq$ 300), for all values of t_a given in table 1, and also the normal cut positions like $t_a = 9m_\pi^2$, $16m_\pi^2$ or $25\,m_\pi^2$. Treating t_a as a free parameter also did not improve the fit significantly. But the introduction of the parameter, $\alpha \neq 0$ and the exponential weight function in the N function drastically reduced the total χ^2 value. The necessity of the exponential weight function for the deuteron magnetic form factor has been emphasized by one of us (Parida 1979). For the lowest anomalous cut position at $t_a = 0{\cdot}0618$ GeV^2, the best fit curve yielded total $\chi^2 = 50{\cdot}4$ with 6 free parameters, corresponding to $\chi^2/DF = 1{\cdot}8$. This fit has been shown by the curve I in figure 2 and the parameters are given in table 2 (case I). Increasing the parameters in the formula did not significantly improve the fit.

To see if the fit can be improved further, we tried different t_a values given in table 2 and also $t_a = 9m_\pi^2$ or $16m_\pi^2$. The fit did not improve much with the next nearest anomalous

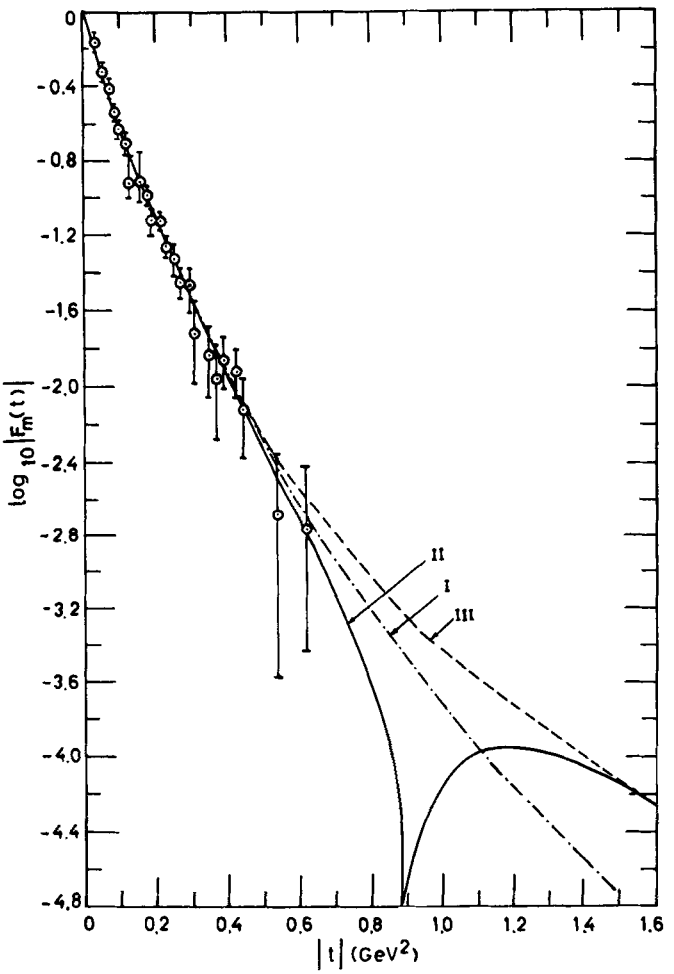

Figure 2. Fits to the ^{3}He magnetic form factor data as a function of various cut positions. Curves I, II and III represent best fits with t_a = 0·0618, 0·175 and 0·247 GeV^2, respectively, in the N-function, but with the two-pion cut in the D-function.

Table 2. Unknown parameters in the N/D representation obtained form analysis of the magnetic form factor data corresponding to curves I, II and III of figure 2. Here g_i's are the coefficients of the optimized polynomial expansion of the N function used for the magnetic form factor.

	I	II	III
t_a (GeV^2)	0·0618	0·1750	0·2470
χ^2/DF	1·80	1·14	1·21
α	2·3730	2·1360	2·7020
a_0 (GeV^2)	0·5696	0·6177	0·6161
a_1	0·5869	0·5840	0·5778
a_2 (GeV^{-2})	0·6609	0·6624	0·6602
e_0 (GeV^2)	0·5696	0·6177	0·6161
e_1 (GeV^2)	−2·6510	−0·2500	−0·4949
e_2 (GeV^2)	0·0086	0·0	0·1381
g_0 (GeV^2)	0·0116	0·5592	0·5341
g_1 (GeV^2)	0·5573	0·0585	0·0726
g_2 (GeV^2)	0·0006	0·0	0·0094

cut at $t_a = 0{\cdot}075$ GeV^2 and yielded $\chi^2/DF = 1{\cdot}7$. As our next choice, we used the next nearest normal three-pion cut, $t_a = 9m_\pi^2 = 0{\cdot}175$ GeV^2, for the function N, and the total χ^2 for the best fit reduced to 30·9 with 5 free parameters, yielding an excellent fit with $\chi^2/DF = 1{\cdot}14$. This fit has been shown as curve II in figure 2 and the parameters are presented in table 2 (case II). As our next step, we used the next nearest anomalous cut at $t_a = 0{\cdot}2475$ GeV^2 for the $N(t)$ function and the best fiit was found to yield total $\chi^2 = 31{\cdot}58$, but with 6 free parameters (one parameter more than the case II) corresponding to a little larger $\chi^2/DF = 1{\cdot}21$. This fit has been shown as curve III in figure 2 and the parameters for this case are represented in table 2 (case III). Increasing the t_a values further was found to increase the total χ^2 value slowly.

The extrapolation of a physical quantity, such as the differential or total cross-section, or the form factor, is a tricky problem whose best solution has been obtained using analyticity and optimized polynomial expansion (Cutkosky and Deo 1968; Cutkosky 1969; Ciulli *et al* 1975). In the present case, the N function has been approximated by the optimized polynomial expansion, but the D function by an effective range type of formula obtainable using dispersion relation. Therefore, the errors in the extrapolated quantities are not minimized and the extrapolation for large $|t|$ values are supposed to be less reliable. Using the results of table 2 and formulas (1)–(7) yields the following asymptotic behaviour for the three fits

$$F_m(t) \underset{t\to\infty}{\to} \frac{(\ln t)^p}{t^n} \exp[-\alpha(\ln t)^2] \tag{11}$$

with $\alpha = 2{\cdot}373$, 2·136 and 2·702 for the fits I, II and III, respectively. For all the three fits $n = 2$, but whereas $p = 2$ for the best fit II, $p = 4$ for the fits I and III.

The extrapolated values of the form factor for smaller $|t|$ regions, where data are not available, are shown in figures 3, 4 and also in figure 2. The presence of a dip at $|t| \simeq 0{\cdot}88$ GeV^2 and a second maximum at $|t| \simeq 1{\cdot}1$–$1{\cdot}3$ GeV^2 is predicted by the best

fit II as shown in figure 2. For the fits I and III, the zeros of the N-function did not exist in the physical region and the dip or the second maximum does not occur for those fits. But since curve III represents an almost equally good fit as curve II, the occurrence of a dip or a second maximum is not a necessary prediction of this analysis.

Extrapolation onto the smaller and larger t values in the time-like regions are shown in figures 3 and 4. Figure 3 exhibits a large slope value of the form factor at $t = 0$ for the lowest value of t_a. Using the parameters of table 2 and the formula (8), we compute the root mean square radius of magnetic moment distribution for ^3He

$$\gamma_m = \begin{cases} 3{\cdot}230 \text{ fm}, & \text{FIT I} \\ 1{\cdot}384 \text{ fm}, & \text{FIT II} \\ 1{\cdot}747 \text{ fm}, & \text{FIT III.} \end{cases} \tag{12}$$

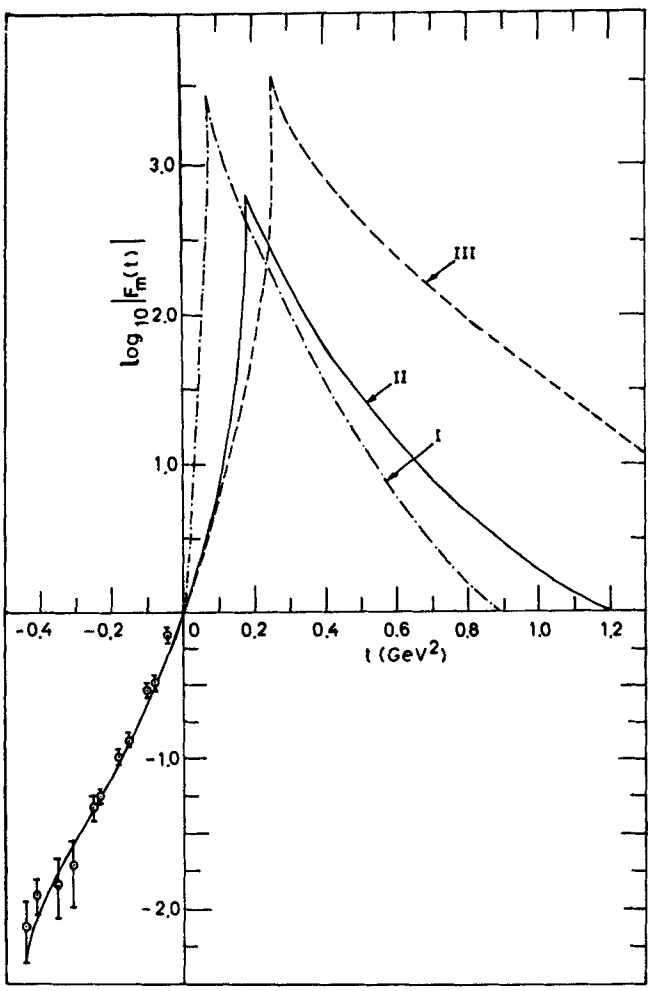

Figure 3. Extrapolation of the ^3He magnetic form factor onto the time-like region with various fits described as curves I, II and III corresponding to figure 2.

In the case of the lowest anomalous cut position, the radius appears to be more than twice the value obtained for the three-pion cut which is closer to the accepted value. Because of this reason, the fit I with the nearest anomalous cut seems to be ruled out as an analytic representation for the magnetic form factor. Using the parameters of table 2 and the formula (8), we also compute the density of magnetic moment distribution $\rho_m(r)$, as a function of r, as shown in figure 5. As compared to the cases with the normal

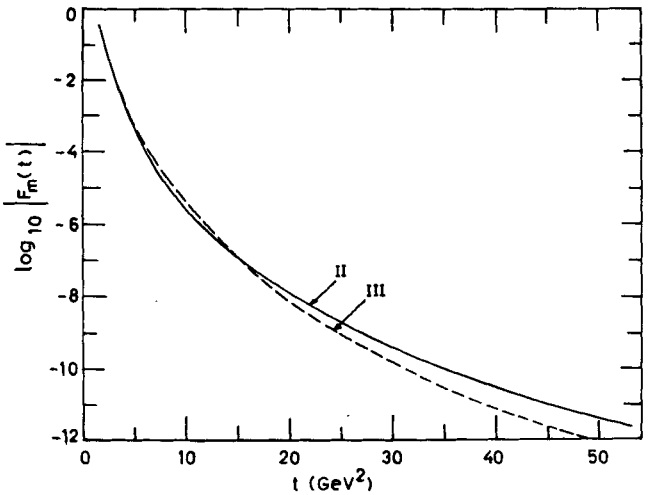

Figure 4. Extrapolation of the fits II and III of figure 2 onto larger $|t|$ values in the spacelike region.

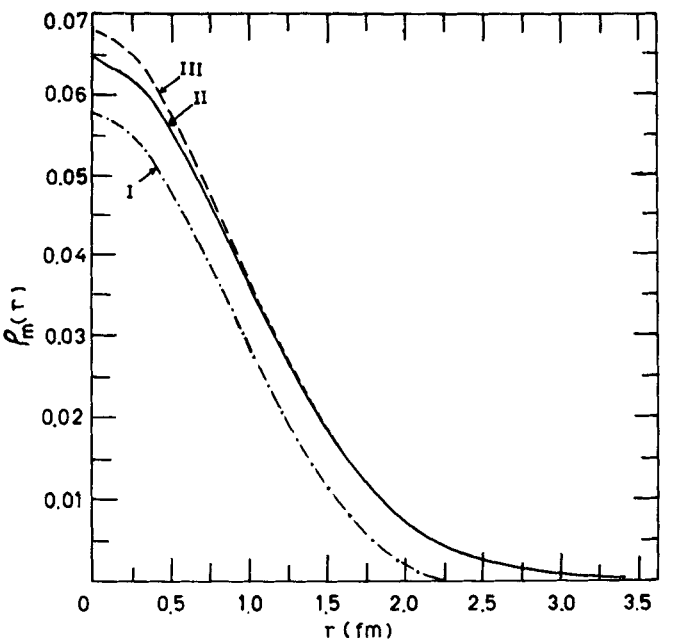

Figure 5. Computation of density of magnetic moment distribution, $\rho_m(r)$ as a function of distance r from the origin corresponding to the fits I, II and III of figure 2.

three-pion cut or the distant anomalous cut (cases II or III), the nearest anamalous cut (case I) yields the density distribution nearly 25 % less for all values of $r < 2{\cdot}5$ fm. For each curve plotted in figure 5, we compute the half density distribution of magnetic moments as

$$\gamma_m h = \begin{cases} 1{\cdot}100 \text{ fm}, & \text{FIT I} \\ 1{\cdot}075 \text{ fm}, & \text{FIT II} \\ 1{\cdot}125 \text{ fm}, & \text{FIT III.} \end{cases} \tag{13}$$

Computed values of physical parameters for the magnetic form factor are shown in table 3 for the three different fits.

4. Analysis of the charge form factor data and extrapolation

We have taken all the available 65 data points with their errors reported by different experimental groups. The D function is chosen in the form (2) with formulas (3) and (4), and the N function is assumed to have the form (7) with formula (6), where t_a was chosen to be an anomalous cut position given in table 1 or the next nearest normal-cut position. As in the case of the magnetic form factor, the exponential weight function with $\alpha > 0$ was found to be essential for any reasonable description of the data. Including the weight function in $N(t)$ we tried to obtain the best possible fits with the nearest anomalous cuts at $t_a = 0{\cdot}01618$ GeV^2 and $0{\cdot}075$ GeV^2. In both cases the fits to the data were found to be very poor. With $t_a = 0{\cdot}0618$ GeV^2 the fit has been presented as curve I in figure 6 which corresponds to total $\chi^2 = 371{\cdot}5$ and $\chi^2/DF = 6{\cdot}2$. With $t_a = 0{\cdot}075$ GeV^2 the fit is similar. However, the total χ^2 reduces drastically by increasing the t_a value. With 6 free parameters the total $\chi^2 = 68{\cdot}8$ (104·5) and $\chi^2/DF = 1{\cdot}16$ (1·77) are obtained for $t_a = 0{\cdot}175$ (0·247) GeV^2 which corresponds to the three-pion (third nearest-anomalous)-cut position. These fits are shown by curves II and III in figure 6. Out of these, curve II is an acceptable best fit which does not predict the presence of a second dip or a third maximum, but fits the first dip and the second maximum very well. The parameters for the curve II are presented in table 4.

Table 3. Different physical quantities of the magnetic form factor obtained using N/D representation and experimental data.

Physical quantities	I	II	III
Root-mean-square radius (fm)	3·230	1·384	1·747
Half-density radius (fm)	1·100	1·075	1·125
Position of first zero (GeV^2)	—	−0·880	—
Position of second maximum (GeV^2)	—	−1·10 to −1·30	—

Table 4. Unknown parameters of the N/D representation of the charge form factor obtained by fitting the experimental data as described in the text for two different cut positions, $t_a = 0{\cdot}175$ GeV^2 and $0{\cdot}19$ GeV^2 of the N-function. Here g_i's are the coefficients of the optimized polynomial expansion used for the N-function.

	II	IV
t_a (GeV^2)	0·175	0·190
χ^2/DF	1·16	1·06
α	2·110	1·9093
a_0 (GeV^2)	0·645	0·6460
a_1	0·0133	0·0837
a_2 (GeV^{-2})	0·605	0·0431
e_0	0·645	0·6460
e_1 (GeV^2)	−0·3266	−0·6102
e_2 (GeV^2)	−0·0587	0·1136
g_0 (GeV^2)	0·5612	0·5017
g_1 (GeV^2)	0·0903	0·1288
g_2 (GeV^2)	−0·0065	0·0155

To know if the fit can be improved further, we treated t_a as a free parameter along with α, e_i and a_m, and found a minimum of total $\chi^2 = 61{\cdot}8$ ($\chi^2/DF = 1{\cdot}06$) with $t_a = 0{\cdot}19$ GeV^2 and 6 free parameters presented in table 4. This fit has been shown by the solid-line curve IV in figure 6. Besides fitting the first dip (second maximum) at $|t| = 0{\cdot}44$ ($0{\cdot}60$) GeV^2, this fit is consistent with the presence of a second dip (third maximum) at $-t = 2{\cdot}4$ ($3{\cdot}0$–$3{\cdot}2$) GeV^2. Thus, although the two fits corresponding to curves II and IV are almost equally acceptable, the latter needs the presence of the second dip and the third maximum. Our analysis on the behaviour of the total χ^2 value as a function of t_a can be summarized in the following manner: as the cut position in the N function starts increasing from $t_a = 0{\cdot}0618$ GeV^2, the total χ^2 decreases, reaches a minimum for $t_a = 0{\cdot}19$ GeV^2 and increases again as t_a is increased beyond this value.

As we have found, there are two almost equally acceptable good fits for the ^{3}He charge form factor with $t_a = 0{\cdot}175$ and $0{\cdot}19$ GeV^2, subject to the limitations that error in the extrapolated quantity increases as we move farther away from the region in the t-plane at which experimental data exist (Cutkosky and Deo 1968; Cutkosky 1969; Ciulli *et al* 1975), the two fits satisfy the asymptotic behaviour of the type

$$F_c(t) \underset{t\to\infty}{\to} \exp[-\alpha(\ln t)^2]\frac{\ln t^4}{t^2}, \tag{13}$$

where $\alpha = 2{\cdot}110$ ($1{\cdot}909$) for the fit II (IV) of figure 6. Using the parameters of the two fits from table 4, we find that both the fits have the first zero of their $N(t)$ function at the experimentally observed dip position, $-t = 0{\cdot}44$ GeV^2. The second zero of the $N(t)$ function for the fit II does not occur in the physical region, but for fit IV, it occurs at $-t = 2{\cdot}40$ GeV^2. Similarly the third maximum for the fit IV appears to exist at $-t = 3{\cdot}0$–$3{\cdot}2$ GeV^2. Since the fits II and IV are almost equally acceptable, the present analysis does not definitely predict the second dip structure. Experimentally, however,

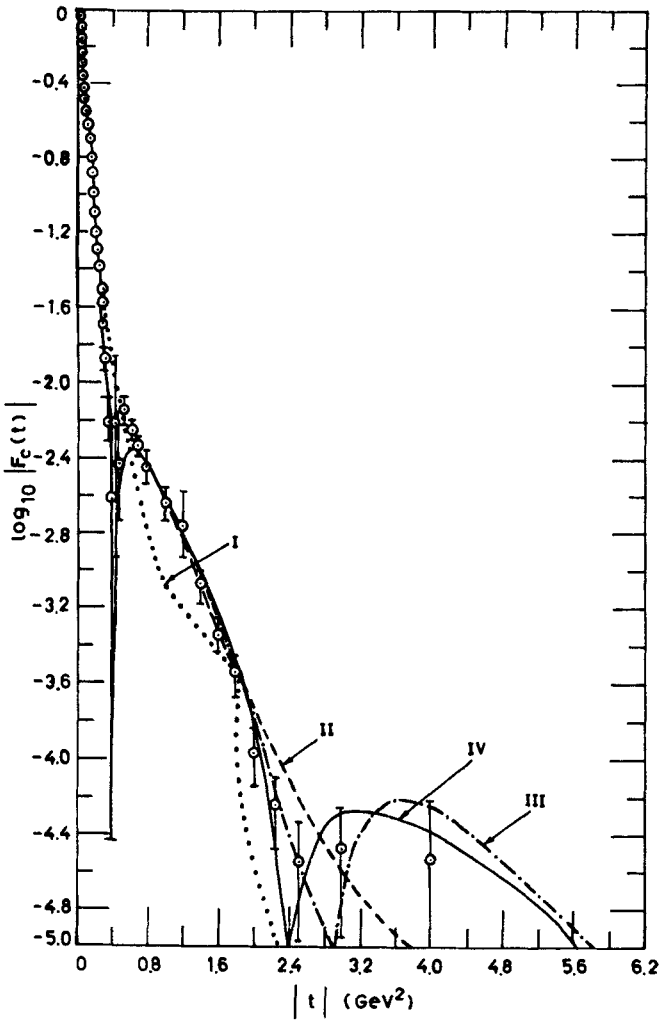

Figure 6. Fits to the available data on ^{3}He charge form factor with the two-pion cut for the D-function. Curves I, II, III and IV represent fits with t_a = 0·0618, 0·175, 0·247 and 0·19 GeV^2, respectively, for the N-function as described in the text.

the data clearly exhibit the existence of a shoulder with rather large errors around $-t$ = 2–3 GeV^2, which has been interpreted as the region of the second dip and third maximum in the fit IV. We suggest that accurate measurements of the charge form factor be carried out for $2{\cdot}0 \leqslant |t| \leqslant 4{\cdot}0$ GeV^2 in order to confirm the presence of the second dip.

Extrapolation of the fit IV onto the larger space-like and time-like t values are shown in figures 7 and 8 respectively. From figure 8 it is clear that the form factor extrapolates smoothly onto the time-like region, producing threshold enhancement at $t_a = 0{\cdot}19$ GeV^2, but having no resonance peaks. The behaviour of fit II, on extrapolation, is similar except that the threshold enhancement in the time-like region occurs at $t_a = (3m_\pi)^2 = 0{\cdot}175$ GeV^2. Using formula (8) and the parameters of table 4 we

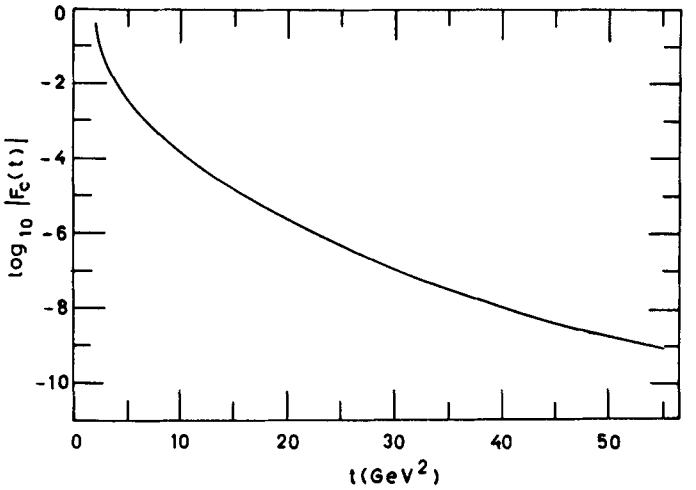

Figure 7. Extrapolation of the solid-line-fit of the ^{3}He charge form factor shown in figure 6 (curve IV) onto larger spacelike $|t|$ values.

calculate the root mean square charge radii for the two fits

$$r_c = \begin{cases} 1{\cdot}875 \text{ fm}, & \text{FIT II} \\ 1{\cdot}966 \text{ fm}, & \text{FIT IV.} \end{cases} \tag{14}$$

Using formulas (1)–(4), (6), (7) and (9), and the parameters from table 4, the charge density $\rho_c(r)$ as a function of r has been calculated for the fit IV and shown in figure 9. The plot of $\rho_c(r)$ vs r for the fit II also shows the same pattern of behaviour. We compute the half density radius for the fit IV to be $r_c^h = 1{\cdot}05$ fm.

The parameters g_i's occurring in the optimized Laguerre polynomial expansion in the N function have been computed using the parameters e_i's and shown in table 4 and comparing formulas (5) and (7); they are found to decrease rapidly as we go over to higher order terms in Z. Although the a_n parameters occurring in the D function for the fit IV are found to decrease with increasing order in t, such a behaviour is not evident in the case of fit II.

5. Summary, discussion and conclusion

This analysis reveals that the proposed N/D method of analytic representation for form factors, which has been successfully tested for isoscalar light nuclei like deuteron and ^{4}He (Parida 1979; Parida *et al* 1983; Agrawalla and Parida 1985), is capable of describing the charge, and magnetic-form-factor data of a nonisoscalar light nucleus like the ^{3}He. Acceptable excellent fits are obtained when the N-function is used to parametrize the three-pion cut, or the anomalous cut at $t_a = 0{\cdot}247$ GeV^2; and, in the former case only, the presence of a dip (secondary maximum) is predicted at $-t = 0{\cdot}88$ $(1{\cdot}1$–$1{\cdot}3)$ GeV^2.

In the case of the charge form factor, two almost equally acceptable fits are found to exist when the N-function is used to parametrize the three-pion cut, or an effective cut

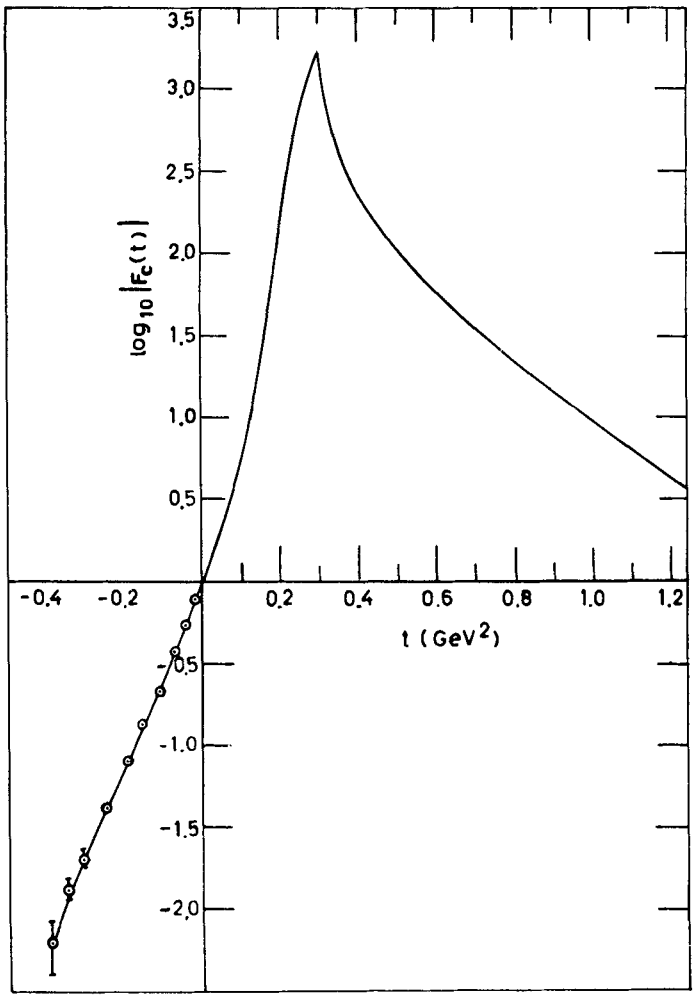

Figure 8. Extrapolation of the ^{3}He charge form factor onto the time-like region using the solid-line fit (curve IV) of figure 6.

very close to it. In the latter case only, the presence of a second dip and a third maximum is predicted to occur. We suggest that accurate charge-form factor measurements in the region $2{\cdot}0 \leqslant -t \leqslant 4{\cdot}0$ GeV^2 be carried out to confirm whether such structures exist.

As we have observed in this and earlier analyses, the presence of the exponential weight function is essential for the nuclear form factors, which contributes a factor $\exp[-\alpha(\ln t)^2]$, to their asymptotic behaviour. It is natural to suppose that since, according to QCD, the hadrons constituting the nucleus are themselves composed of coloured quarks, the quark form factor should occur as a factor in the actual nuclear form factor at least for large $|t|$ values. In fact such a type of asymptotic behaviour of the quark form factor in the leading logarithmic order has been calculated using QCD and asymptotic dynamics (Dahman *et al* 1980; Kulish *et al* 1970, 1971).

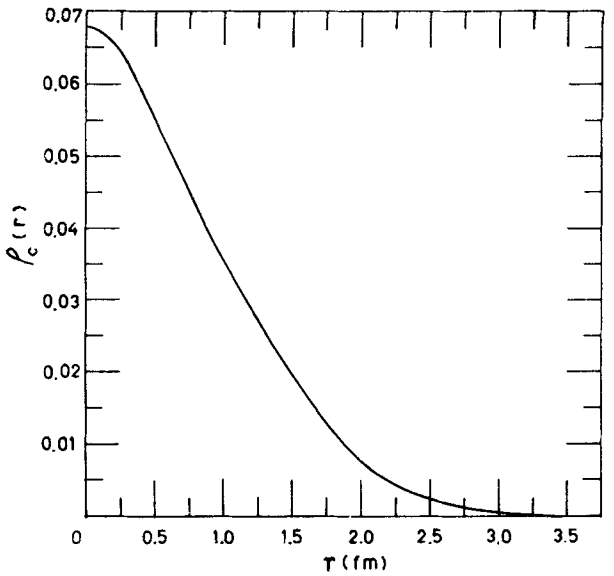

Figure 9. Computation of charge density $\rho_c(r)$ as a function of r for ^{3}He using the solid-line fit (curve IV) of figure 6.

References

Agrawalla K N and Parida M K 1985 *Phys. Rev.* **D32** 2359
Ciulli S 1969 *Nuovo Cimento* **A61** 787
Ciulli S, Pomponiu and Sabba Stefanescu I 1975 *Phys. Rep.* **C17** 133
Cutkosky R E 1969 *Ann. Phys. (N.Y.)* **54** 110
Cutkosky R E and Deo B B 1968 *Phys. Rev.* **174** 1859
Dahman H D and Steiner F 1980 DESY preprint DESY 80/37
Deo B B 1974 *Indian J. Phys.* **48** 705
Deo B B and Parida M K 1971 *Phys. Rev. Lett.* **26** 1609
Deo B B and Parida M K 1973 *Phys. Rev.* **D8** 2939
Deo B B and Parida M K 1974 *Phys. Rev.* **D9** 2068
Eden R J, Landshoff P V, Olive D I and Polkinghorne J C 1966 *The analytic S-matrix* (Cambridge: University Press)
Frosch R F, McCarthy J S, Rand R E and Yearian M R 1967 *Phys. Rev.* **160** 874
Hamilton J 1968 Lecture given at the Neils Bohr Institute, NORDITA (Nordita Publications)
Kulish P P and Faddeev L D 1970 *Theor. Maten Fiz.* **4** 153
McAllister R W and Hofstadter R 1956 *Phys. Rev.* **102** 851
McCarthy J S, Sick I and Whitney R R 1977 *Phys. Rev.* **C15** 1396
Parida M K 1979 *Phys. Rev.* **D19** 3320
Parida M K, Patel S and Agrawalla K N 1983 *Phys. Rev.* **D27** 1187